

AFOSR 66-0569

AF EOAR 63-58

SR-2

August 1965

TECHNION RESEARCH & DEVELOPMENT
FOUNDATION, HAIFA, ISRAEL

SCIENTIFIC REPORT No. 2

**FURTHER REMARKS ON THE EFFECT OF ECCENTRICITY
OF STIFFENERS ON THE GENERAL INSTABILITY OF
STIFFENED CYLINDRICAL SHELLS**

Josef Singer, Menahem Baruch and Ovadia Harari

Technion - Israel Institute of Technology,
Department of Aeronautical Engineering.

Haifa, Israel.

TAE REPORT No. 42

CLEARINGHOUSE FOR FEDERAL SCIENTIFIC AND TECHNICAL INFORMATION		
Hardcopy	Microfilm	
\$ 2.00	\$ 0.50	35 pp. as
ARCHIVE COPY		

Coile /

AUGUST 1965

SCIENTIFIC REPORT No. 2

FURTHER REMARKS ON THE EFFECT OF ECCENTRICITY
OF STIFFENERS ON THE GENERAL INSTABILITY OF
STIFFENED CYLINDRICAL SHELLS

Josef Singer, Menahem Baruch and Ovadia Harari
Technion - Israel Institute of Technology
Department of Aeronautical Engineering
Haifa, Israel.

TAE REPORT No. 42

S U M M A R Y

The analysis of the general instability of stiffened cylindrical shells under hydrostatic pressure carried out earlier is continued in order to study the inversion of the eccentricity effect. 250 typical shells of varying geometries are considered. The results show that the inversion of the eccentricity effect is practically independent of the geometry of the rings but depends very strongly on the shell geometry parameter Z . A range of inversion is found.

A detailed physical explanation of the causes of the eccentricity effect and its inversion is proposed.

TABLE OF CONTENTS

	<i>P a g e</i>
SUMMARY	I
LIST OF FIGURES	III
LIST OF SYMBOLS	IV
SECTION 1. INTRODUCTION	1
SECTION 2. THE EFFECT OF ECCENTRICITY	2
SECTION 3. PHYSICAL EXPLANATION	4
SECTION 4. NUMERICAL RESULTS AND DISCUSSION	8
SECTION 5. CONCLUSIONS	11
ACKNOWLEDGEMENT	
REFERENCES	12

LIST OF FIGURES

- Fig. 1 - Notation
- Fig. 2 - Variation of Circumferential strain with shell geometry
- Fig. 3 - The primary eccentricity effect
- Fig. 4 - The secondary eccentricity effect
- Fig. 5 - Variation of eccentricity effect with shell parameter Z
- Fig. 6 - Influence of ring area and moment of inertia on stiffening of shell
- Fig. 7 - Effect of magnitude of eccentricity on stiffening of shell
- Fig. 8 - Variation of eccentricity effect with magnitude of eccentricity
- Fig. 9 - Variation of stiffening of shell with ring area and moment of inertia .

IV

S Y M B O L S

A_n	- coefficient of axial displacement
A_1	- cross-sectional area of stringer
A_2	- cross-sectional area of frame (ring)
a	- distance between frames (rings)
B_n	- coefficient of circumferential displacement
b	- distance between stringers
C_n	- coefficient of radial displacement
D	- $[Eh^3 / 12(1-\nu^2)]$
E, E_1, E_2	- moduli of elasticity of shell, stringers and frames, respectively
e_1, e_2	- distance between centroid of stiffener cross-section and middle surface shell, positive when inside (see Fig. 1).
G_1, G_2	- shear moduli of stringers and frames, respectively
h	- thickness of shell
I_{11}, I_{22}	- moment of inertia of stiffener cross-section about its centroidal axis
I_{01}, I_{02}	- moment of inertia of stiffener cross-section about the middle surface of the shell
I_{t1}, I_{t2}	- torsion constant of stiffener cross-section
L	- length of shell between bulkheads
$M_x, M_\phi, M_{x\phi}$	- moment resultants acting on element
\bar{M}_x, \bar{M}_ϕ	- geometrical bending stiffness of stringer-shell or ring-shell combination

$N_x, N_\phi, N_{x\phi}$	— membrane force resultants acting on element
n	— integer
$N_{x0}, N_{\phi0}, N_{x\phi0}$	— prebuckling membrane force resultants
p	— hydrostatic pressure
R	— radius of shell
t	— number of circumferential waves
u	— non-dimensional axial displacement ($=u^*/R$)
u^*	— axial displacement
v	— non-dimensional circumferential displacement ($=v^*/R$)
v^*	— circumferential displacement
w	— non-dimensional radial displacement ($=w^*/R$)
w^*	— radial displacement
x	— non-dimensional axial co-ordinate ($=x^*/R$)
x^*	— axial co-ordinate
Z	— $(1-\nu^2)^{1/2} (L/R)^2 (R/h)$
z	— Non-dimensional radial co-ordinate ($=z^*/R$)
z^*	— radial co-ordinate
\bar{z}_1, \bar{z}_2	— distance of the centroid of the stringer-shell, or ring-shell combination from the middle surface (see Fig. 3a).
β	— $\pi K/L$

VI

ϵ_x	- $\ddot{u}_{,x}$	} middle surface strains
ϵ_ϕ	- $v_{,\phi} - w$	
$\gamma_{x\phi}$	- $u_{,\phi} + v_{,x}$	
ζ_1	- $(E_1 A_1 e_1 R/bD)$	
ζ_2	- $(E_2 A_2 e_2 R/aD)$	
η_{01}	- $(E_1 I_{01}/bD)$	
η_{02}	- $(E_2 I_{02}/aD)$	
η_{t1}	- $(G_1 I_{t1}/bD)$	
η_{t2}	- $(G_2 I_{t2}/aD)$	
κ_x	- $w_{,xx}$	} non dimensional changes of curvature and twist of the middle surface
κ_ϕ	- $w_{,\phi\phi}$	
$\kappa_{x\phi}$	- $w_{,x\phi}$	
λ_p	- $(R^3/D)p$	
μ_1	- $(1-\nu^2) (E_1 A_1/Ebh)$	
μ_2	- $(1-\nu^2) (E_2 A_2/Eah)$	
ν	- poisson's ratio	
ϕ	- circumferential co-ordinate	
X_1	- $(1-\nu^2) (E_1 A_1 e_1/EbhR)$	
X_2	- $(1-\nu^2) (E_2 A_2 e_2/EahR)$	

Subscripts following a comma indicate differentiation.

1. I N T R O D U C T I O N

In Reference [1] the general instability of simply supported cylindrical shells under hydrostatic pressure was analysed by considering the "distributed" stiffness of rings and stringers separately and taking into account their eccentricity. It was concluded there that rings on the inside of the shell yield higher general instability pressures than rings on the outside. For stringers, which are much less effective in stiffening against hydrostatic pressure, the effect of eccentricity was found to "be opposite", outside stringers yielding higher critical pressures than inside stringers. Similar eccentricity effects were found for conical shells.[2]

During recent calculations of the general instability of conical shells with non-uniformly spaced stiffeners under hydrostatic pressure [3], the ring eccentricity effect was found to be inverted for some very short and thick shells. The reason for this inversion became clear after some further study of the general instability of stiffened cylindrical and conical shells. More extensive computations seemed desirable in order to obtain a better feeling for the influence of the geometric parameters of the shell on the eccentricity effect.

The results of these computations for a large number of typical shells show that the inversion of the eccentricity effect is practically independent of the geometry of the rings but depends very strongly on the shell geometry. Furthermore, if the geometry of the shell is represented by the well known non-dimensional Batdorf parameter $Z = (1-\nu^2)^{1/2}(L^2/Rh)$, a "range of inversion" is found.

It should be pointed out that the inversion of the eccentricity effect for short shells was also observed in very recent computations carried out by Mc Elman et al.[4] and by Geier and Seggelke [5], but no general conclusions about the geometrical parameters which determine the inversion were reached.

The study of the influence of the geometric parameters on the eccentricity effect motivated a re-evaluation of the physical explanation of the phenomena, which resulted in a much clearer picture of the buckling behavior of stiffened cylindrical shells.

For clarity, the main assumptions made in [1] and [2] are repeated here:

- a) The stiffeners are "distributed" over the whole surface of the shell.
- b) The normal strains $\epsilon_x(z)$ and $\epsilon_\phi(z)$ vary linearly in the stiffener as well as in the sheet. The

normal strains in the stiffener and in the sheet are equal at their point of contact.

- c) The stiffeners do not transmit shear. The shear membrane force $N_{x\phi}$ is carried entirely by the sheet
- d) The torsional rigidity of the stiffener cross section is added to that of the sheet (the actual increase in torsional rigidity is larger than that assumed).

Note also that the middle surface of the shell is chosen as reference line.

2. THE EFFECT OF ECCENTRICITY

In order to study the effect of the eccentricity of stiffeners one has to examine the expressions for the forces and moments acting on an element of the stiffened shell, Eqs. (5) and (6) of [1]. After substitution of the strain-displacement and curvature-displacement relations, Eqs. (3) and (4) of [1], the forces and moments become

$$\begin{aligned} N_x &= [Eh/(1-\nu^2)] [u_{,x}(1+\mu_1) + \nu(v_{,\phi} - w) - \chi_1 w_{,xx}] \\ N_\phi &= [Eh/(1-\nu^2)] [(v_{,\phi} - w)(1+\mu_2) + \nu u_{,x} - \chi_2 w_{,\phi\phi}] \\ N_{x\phi} = N_{\phi x} &= [Eh/2(1+\nu)] (u_{,\phi} + v_{,x}) \end{aligned} \quad (1)$$

$$\begin{aligned} M_x &= -(D/R) [w_{,xx}(1+\eta_{01}) + \nu w_{,\phi\phi} - \zeta_1 u_{,x}] \\ M_\phi &= -(D/R) [w_{,\phi\phi}(1+\eta_{02}) + \nu w_{,xx} - \zeta_2 (v_{,\phi} - w)] \\ M_{x\phi} &= +(D/R) [(1-\nu) + \eta_{11}] w_{,x\phi} \\ M_{\phi x} &= -(D/R) [(1-\nu) + \eta_{12}] w_{,x\phi} \end{aligned} \quad (2)$$

where μ_1 , μ_2 , η_{01} , η_{02} , η_{11} and η_{12} are the changes in stiffnesses due to stringers and frames and χ_1, χ_2 , ζ_1 and ζ_2 are the changes in stiffnesses caused by the eccentricities of the stringers and rings, as in [1]. Since the analysis is concerned with instability, u , v and w are the additional displacements during buckling, and as in [1] they are non-dimensional, the physical displacements having been divided

by the radius of the shell.

The usual simple support boundary conditions are assumed as in [1] and

$$\begin{aligned} u &= A_n \sin t\phi \cos n\beta x \\ v &= B_n \cos t\phi \sin n\beta x \\ w &= C_n \sin t\phi \sin n\beta x \end{aligned} \quad (3)$$

are the displacements which solve the Donnell type stability equations for general instability, Eqs.(12) of [1], in the presence of these boundary conditions.

In the case of rings, the effect of their eccentricity on the forces is represented by the term $-\chi_2 w, \phi\phi$ in the second of Eqs.(1), and on the moments by the term $-\zeta_2 (v, \phi - w)$ and $\eta_{02} w, \phi\phi$ (since $\eta_{02} = (E_2 I_{22}/aD) + (E_2 A_2 e_2^2/aD)$) in the second of Eqs.(2). Note that the sign of the eccentricity affects only the terms with χ_2 and ζ_2 . For internal rings (positive e_2) χ_2 and ζ_2 are positive.

The eccentricity effect is the result of coupling between moments and membrane forces, and for ring stiffened shells the circumferential middle surface strain, $\epsilon_\phi = (v, \phi - w)$, is found to be the major coupling factor. In Fig.2 the variation of ϵ_ϕ with Z is plotted for a typical ring geometry, $(A_2/ah) = 0.5$, $(I_{22}/ah^3) = 5$, and $(e_2/h) = \pm 5$. It should be pointed out that the ring geometry represents relatively strong rings with a large eccentricity. The relative circumferential middle surface strain (ϵ_ϕ/C_n) is small for long and thin shells, but becomes large for short and thick shells (small Z), in which the membrane forces contribute significantly to the resistance against buckling. (ϵ_ϕ/C_n) is always negative for inside rings (positive e_2) and positive for outside rings (negative e_2), except for very small Z . For long and thin shells the magnitude of (ϵ_ϕ/C_n) is larger for outside rings than for inside ones. With decreasing Z the ratio of $(|\epsilon_\phi \text{ outside}| / |\epsilon_\phi \text{ inside}|)$ decreases and after a certain value of Z becomes less than unity. Eventually at a very small Z , (ϵ_ϕ/C_n) for outside rings even changes its sign. The change from larger $|\epsilon_\phi/C_n|$ for outside rings to larger $|\epsilon_\phi/C_n|$ for inside rings occurs at the same Z at which the inversion of the total eccentricity effect is found. Hence one observes that the eccen-

tricity effect is closely related to the behavior of ϵ_ϕ .

For long and thin ring stiffened shells M_ϕ is the prime factor determining the resistance of the shell to buckling. From the second of Eqs.(2) one sees that the magnitude of M_ϕ depends primarily on $w_{,\phi\phi} \eta_{02} - \zeta_2 (v_{,\phi} - w)$. With increasing eccentricity of rings e_2 , η_{02} increases rapidly but independently of the sign of e_2 . The second term $-\zeta_2 (v_{,\phi} - w)$ reduces M_ϕ for both inside or outside rings (except for very small Z). This occurs since $(w_{,\phi\phi}/w)$ is negative and for inside rings (see Fig.2), positive ζ_2 , $(v_{,\phi} - w)/w$ is also negative; whereas for outside rings, negative ζ_2 , $(v_{,\phi} - w)/w$ is positive. However, due to the larger magnitude of $|\epsilon_\phi/C_n|$ for outside rings, the reduction in M_ϕ is larger for negative e_2 and the stiffness of the shell is therefore smaller. Hence the usual eccentricity effect of higher loads with inside rings is explained. Note that as the first term, which does not depend on the sign of the eccentricity, dominates, the eccentricity effect cannot be very pronounced as is indeed found in all the calculations (the largest effect encountered was 25% for a shell with extremely large eccentricity).

For shorter and thicker shells, the effect decreases and eventually inverts when the reduction in M_ϕ becomes larger for inside rings than outside ones. For very small Z , when (ϵ_ϕ/C_n) for outside rings changes sign, M_ϕ is not only reduced less but is actually increased. Hence pronounced eccentricity effects can be expected and are indeed found in the calculations. It should be pointed out that, although the membrane forces contribute significantly to the resistance of shells with small Z , the eccentricity effect is primarily caused by changes in M_ϕ .

3. PHYSICAL EXPLANATION

If one aims at a physical explanation of the effect of eccentricity of rings on the instability of cylindrical shells, without direct reference to the mathematical formulation, one finds that the effect is made up of two opposing contributions. The primary contribution is the effect of the membrane stresses in the shell on the bending stiffness of the shell-stiffener combination, and the opposing secondary contribution is the effect of the bending strains on the membrane stresses in the shell.

The primary effect in rings is similar to that causing the more spectacular eccentricity effects in stringer stiffened axially compressed cylinders, whereas the secondary effect is more prominent in rings.

An explanation for the considerable increase in buckling load under axial compression with outside stringers, which has been demonstrated experimentally by many investigators (see [6] -[9]), has recently been given by Thielemann and Esslinger [10]. One could extend the argument of [10] to rings; however, here a more complete explanation is presented which covers both the primary and the secondary contributions of the eccentricity effect for any stiffener.

The total geometrical bending stiffness of the combined ring-shell cross-section is not affected by the place of the rings and is equal for outside and inside stiffening. Now, as a result of the initial curvature of the shell additional membrane forces appear in it during buckling. If one considers the circumferential membrane forces this is immediately apparent, since for outward buckles the shell has to lengthen and tensile forces arise, while for inward buckles the shell has to shorten and compressive forces arise.

A relation between the axial and circumferential membrane forces is obtained by differentiating the first two stability equations

$$\begin{aligned} N_{x,x} + N_{x\phi,\phi} &= 0 \\ N_{\phi,\phi} + N_{x\phi,x} &= 0 \end{aligned} \quad (4)$$

with respect to x and ϕ

$$N_{x,xx} = N_{\phi,\phi\phi} \quad (5)$$

By substitution of the assumed displacements, Eqs.(3), into Eq.(5) this relation between the membrane forces becomes

$$n^2 \beta^2 N_x = t^2 N_\phi \quad (6)$$

As mentioned, N_ϕ is compressive in a positive (inward) wave and tensile in a negative wave. From Eq.(6) it is seen that N_x follows N_ϕ at every point of the shell, and that for long shells N_x is much

larger than N_ϕ (since for hydrostatic pressure $n = 1$ and in long shells $\beta < 1$ while t is always larger than 2).

It should be noted that Eq.(6) is true only for the classical simple support boundary conditions assumed here

$$\begin{aligned} v &= 0 \\ w &= 0 \\ N_x &= 0 \\ M_x &= 0 \end{aligned} \quad \text{at } x = 0, L/R \quad (7)$$

For other boundary conditions similar relations between N_x and N_ϕ can probably be obtained, but the details require further study.

In Figs. 3a to 3d \bar{M}_ϕ represents the geometrical bending stiffness of the cross-section of the ring-shell combination. It is the moment necessary to produce a certain change in curvature. The geometrical stiffness \bar{M}_ϕ is equal for the inside and outside ring-shell combinations.

However, due to the circumferential membrane force acting in the shell, the actual total bending stiffness of the cross-section is changed. For a ring-shell combination with inside rings the actual total bending stiffness is (See Figs. 3a and 3c)

$$M_\phi^{in} = \bar{M}_\phi - \bar{z}_2 N_\phi^{in} \quad (8)$$

where M_ϕ^{in} is the actual moment necessary to produce the same change of curvature that \bar{M}_ϕ would produce without the membrane force N_ϕ^{in} .

In the same manner, the actual bending stiffness for the cross-section with outside rings is

$$M_\phi^{out} = \bar{M}_\phi + \bar{z}_2 N_\phi^{out} \quad (9)$$

where again M_ϕ^{out} is the actual moment necessary to produce the same change of curvature which \bar{M}_ϕ would produce without the membrane force N_ϕ^{out} .

From Eqs.(8) and (9) it can be seen that the actual bending stiffness for outside stiffening is

larger than that for inside stiffening. This is the primary eccentricity effect. There is, however, another opposing secondary effect which will now be examined.

Consider a shell with inside rings. In a positive wave, the moment M_ϕ produces in the shell an additional compressive strain in the circumferential direction. Due to Poisson's effect (ν), an axial strain appears in the sheet, giving rise to an additional compressive membrane force, ΔN_x , in the axial direction, which resists this strain. From equilibrium considerations, Eq.(6), ΔN_x is accompanied by an additional compressive membrane force ΔN_ϕ , in the circumferential direction. This additional compressive force has a radial component which resists radial deformation (Fig.4a). On the other hand, for outside rings the additional force ΔN_ϕ is tensile and therefore assists deformation (Fig.4b). In a negative wave (Figs. 4c and 4d) the same argument applies and the additional membrane force ΔN_ϕ resists the deformation for inside rings, whereas it assists it for outside rings.

The effect of eccentricity of rings can therefore be summarised as follows:

1. Primary effect — outside rings increase the actual bending stiffness in the circumferential direction more than inside rings.
2. Secondary effect — inside rings increase the actual extensional stiffness in the circumferential direction more than outside rings.

Now, for long cylinders N_ϕ is very small and the difference in the actual bending stiffness in the circumferential direction for inside and outside rings, Eqs.(8) and (9), is also very small. On the contrary, M_ϕ is relatively large, and therefore the ΔN_ϕ produced by it is important. Hence for long cylinders, the critical load for inside ring stiffening is larger than that for outside ring stiffening. It should be remembered that this is due to the Poisson's effect (ν). If the Poisson's effect is neglected ($\nu = 0$), outside ring stiffening yields higher critical loads than inside ring stiffening even for long cylinders (See Table 4).

For short cylinders N_ϕ begins to increase but M_ϕ is still an important factor. The difference in the actual bending stiffness increases (See Eqs.(8) and (9)) and the critical load for outside rings is much larger than that for inside rings.

The behavior of a stringer stiffened shell can be explained in a similar manner. As for ring-stiffening, the actual bending stiffnesses in the axial direction for stringer stiffening are

$$\begin{aligned}
 M_x^{in} &= \bar{M}_x - \bar{z}_1 N_x^{in} \\
 M_x^{out} &= \bar{M}_x + \bar{z}_1 N_x^{out}
 \end{aligned}
 \tag{10}$$

where \bar{M}_x represents the geometrical stiffness of the cross-section of stringer-shell combinations and is equal for inside and outside stringer stiffening, and M_x^{in} and M_x^{out} represent the actual bending stiffness for inside and outside stringers.

Again, due to the moment, M_x , and Poisson's effect, ν , there is another opposing secondary effect. Therefore the effect of eccentricity of stringers can be summarized as follows:

1. Primary effect — outside stringers increase the actual bending stiffness in the axial direction more than inside stringers.
2. Secondary effect — inside stringers increase the extensional stiffness in the circumferential direction more than outside stringers.

However, for stringer-stiffened shells no inversion of the eccentricity effect has been observed. This difference between the eccentricity effect in ring-stiffened shells and stringer-stiffened ones can be explained by consideration of the magnitudes of the governing forces and moments. In ring-stiffened shells, N_ϕ diminishes rapidly with (L/R) while M_ϕ remains relatively large. Hence ΔN_ϕ caused by M_ϕ is large compared with N_ϕ for long shells and the secondary effect can dominate, causing inversion of the eccentricity effect. In stringer-stiffened shells, on the other hand, N_x remains relatively large even for long shells, while M_x is relatively small. Hence ΔN_x caused by M_x is small compared with N_x even for long shells, and the secondary effect (which depends on the resulting small ΔN_ϕ) cannot become significant enough to cause inversion.

4. NUMERICAL RESULTS AND DISCUSSION

The critical pressures for general instability under hydrostatic and lateral pressure were computed for 250 ring and stringer stiffened shells covering a wide range of shell and stiffener geometries. In the numerical work most of the shells are ring-stiffened, since stringers are very inefficient under hydrostatic

or lateral pressure (see [1]).

In Fig.5 the ratio (p^{out}/p^{in}) (where p^{in} is the critical pressure for inside ring stiffeners and p^{out} that for outside ones) is plotted as a function of the Batdorf parameter $Z = (1-\nu^2)^{1/2} (R/h) (L/R)^2$, which defines the shell geometry. A range of Z is found in which the inversion of the eccentricity effect occurs. It spreads between $100 < Z < 500$, or in other words, for $Z > 500$ p^{in} is always larger than p^{out} and for $Z < 100$, p^{in} is smaller than p^{out} . Shells with different rings are plotted in the same figure, and it can be seen that the inversion of the eccentricity effect depends mainly on the shell geometry. Variations in the geometry of rings, even from very weak rings to very strong ones, for Z above 300, result in a very small change in the (p^{out}/p^{in}) ratio. On the other hand, in very short and thick shells, changes in the geometry of rings yield noticeable differences in the (p^{out}/p^{in}) ratio (Fig.5).

These extensive calculations, as well as the physical explanation, show clearly the importance of the shell geometry for the direction of the eccentricity effect. Hence Crawford's conclusion, [11], that under hydrostatic pressure, rings on the outside of the shell will result in higher strength than when they are on the inside is not general and applies only to a certain range of shell geometries.

As mentioned in the introduction, the eccentricity effect is made up basically from two opposing contributions: the primary and the secondary effect. The primary effect causes higher buckling loads for outside ring stiffened shells. The percentage difference (p^{out}/p^{in}) decreases with Z , which is consistent with the physical explanation, since for long and thin shells, the influence of the membrane forces on the effective bending stiffness of the ring-sheet combination diminishes. As $Z \rightarrow \infty$ (very long shells unaffected by boundary conditions) the primary effect tends to zero. The opposing secondary effect is due to Poisson's ratio. It also tends to zero as $Z \rightarrow \infty$, since the membrane forces are zero in the limit, but more slowly than the primary effect. The reason for the slower rate of diminishing is apparent from the physical explanation, if one remembers that the secondary effect is caused by M_ϕ , which does not disappear in long shells. In Table 4 the effect of Poisson's ratio on the eccentricity effect was checked numerically for two typical shells. By assuming $\nu = 0$ the secondary effect is eliminated, and one obtains $p^{out} > p^{in}$ even for long shells ($R/h = 2000$ $L/R = 2$). In checking the other limit, by taking $\nu = 0.5$, the secondary effect is enhanced and p^{in} becomes 30% greater than p^{out} . By comparing the results obtained for $\nu = 0$ in the long and short shells one clearly observes the asymptotic behavior

of the primary effect with Z .

In Table 5, ring and stringer stiffening is compared for a large range of shell geometries. The longer the shell, the less effective are stringers in stiffening against buckling under hydrostatic pressure. For very short shells stringers and rings are equally effective as stiffeners. This can be explained if one remembers that hydrostatic pressure is composed of axial and lateral components. In short shells, both components affect buckling to the same extent. Now, rings are more effective against lateral pressure than stringers. On the other hand, axial pressure is resisted much better by longitudinal stiffeners than by rings. Hence in the case of hydrostatic pressure, rings and stringers stiffen by the same amount.

In Table 2, the effect of ring geometry is studied for different shell configurations, and the results are plotted in Figs. 6-7. There one sees clearly that the buckling load depends on the combined shell geometry parameter Z and not on the separate parameters R/h and L/R . One also observes that for different rings the inversion occurs almost at the same value of Z . There is only a very slight shift in the inversion with ring geometry. For stronger stiffeners inversion occurs at a higher Z , for example

$$A_2/ah = 0.8 \quad I_{22}/ah^3 = 8 \quad Z_{INV} \approx 400$$

$$A_2/ah = 0.1 \quad I_{22}/ah^3 = 1 \quad Z_{INV} \approx 180$$

In Fig. 8, the variation of the eccentricity effect with magnitude of eccentricity was studied. The higher $|e_2|$, the stiffer the shell is against buckling. Therefore one expects the same behavior as that found for increasing moment of inertia (I_{22}/ah^3) in Fig. 9. For short shells this behavior is indeed observed, as monotonous rise of (p^{out}/p^{in}) with $|e_2|$. However, when longer and thinner shells are considered, a different behavior appears. On varying the magnitude of $|e_2|$ for a certain shell geometry, p^{out} is first found to be smaller than p^{in} . On increasing $|e_2|$, p^{out}/p^{in} passes through a minimum and starts to rise again, and eventually an inversion of the eccentricity effect occurs.

For short and thick shells a comparison between buckling under hydrostatic and lateral pressure was made (Table 3). This comparison was carried out in order to eliminate any doubts about the cause of the inversion of the eccentricity effect. In the early stages of the work it was suspected that the axial component of the hydrostatic pressure is the cause of the inversion, since inversion occurs only in short

shells. However, the calculations for a typical ring geometry (Table 3) showed that inversion occurs even with lateral pressure. The physical explanation arrived at later proved that this was to be expected.

5. CONCLUSIONS

The results of calculation for 250 typical cylindrical shells show that for shells with $Z < 100$ outside rings are more efficient stiffeners against hydrostatic and lateral pressure than inside rings, whereas for $Z > 500$, shells with inside rings are stronger. Stringers are much less efficient as stiffeners against hydrostatic pressure, except for very short shells. Outside stringers are better than inside ones.

ACKNOWLEDGEMENT

The authors would like to thank Mr. E. Glinert for assistance with the programming, and Mrs. J. Stern for assistance with the computations and the staff of the Technion Computing Center for their valuable help.

REFERENCES

1. Baruch, M. and Singer, J. Effect of Eccentricity of Stiffeners on the General Instability of Stiffened Cylindrical Shells Under Hydrostatic Pressure. *Journal of Mechanical Engineering Science*, Vol.5, No.1, p.23, March 1963.
2. Baruch, M. and Singer, J. General Instability of Stiffened Circular Conical Shells Under Hydrostatic Pressure. *The Aeronautical Quarterly*, Vol.26, Part 2, p.187, May 1965. Also TAE Report 28, Technion Research and Development Foundation, Haifa, Israel, July 1963.
3. Baruch, M., Singer, J. and Harari, O. General Instability of Conical Shells With Non-Uniformly Spaced Stiffeners Under Hydrostatic Pressure, *Proceedings of the 7th Israel Annual Conference on Aviation and Astronautics*, February 1965, p.62. Also TAE Report 37, Technion Research and Development Foundation, Haifa Israel, December 1964.
4. Mc Elman, J.A., Mikulas, M.M. and Stein, M. Static and Dynamic Effects of Eccentric Stiffening of Plates and Cylindrical Shells, *Presented at the 2nd AIAA Annual Meeting and Technical Display*, San Francisco 26-29 July 1965.
5. Geier, B. and Seggelke, P. Das Beulverhalten versteifter Zylinderschalen. Teil 2. Beullasten bei axial-symmetrischer Belastung (to be published in *Zeitschrift für Flugwissenschaften*)
6. Houghton, D.S. and Chan, A.S.L. Design of a Pressurised Missile Body, *Aircraft Engineering*, Vol. 32, No.381, November 1960, p.320.
7. Card, M.F. Preliminary Results of Compression Tests on Cylinders with Eccentric Longitudinal Stiffeners, NASA TM X - 1004, September 1964.
8. De Luzio, A.J., Stuhlman, C.E. and Almroth, B.O. Influence of Stiffener Eccentricity and End Moment on the Stability of Cylinders in Compression, *Presented at the AIAA 6th Struc-*

tures and Materials Conference, Palm Springs, 5 - 7 April 1965.

9. Garkisch, H.D., Geier, B. and Seggelke, P. Beulversuche an längsversteiften Zylinderschalen (to be published as a DLR - FB)
10. Thielemann, W. and Esslinger, M. Ueber den Einfluss der Exzentrizität von Längssteifen auf die axiale Beullast dünnwandiger Kreiszyinderschalen (to be published as a DLR - FB)
11. Crawford, R.F. Effects of Asymmetric Stiffening on Buckling of Shells. Presented at the 2nd AIAA Annual Meeting and Technical Display, San Francisco 26 - 29 July 1965.

TABLE. 1

GENERAL INSTABILITY PRESSURES OF RING STIFFENED SHELLS
EFFECT of SHELL GEOMETRY

$$A_2/ah = .5 \quad I_{22}/ah^3 = 5 \quad e_z/h = .5$$

CASE	R/h	L/R	Z	λ_0 UNSTIFFENED	λ_{cr}				λ^+/λ_0	λ^-/λ_0	λ^-/λ^+
					$+e_z$ inside	t	$-e_z$ outside	t			
1	50	0.5	11.98	173.2	896.8	3	1768	3	5.178	10.21	1.972
2		1.0	47.70	70.48	1216	3	1707	3	15.50	21.75	1.404
3		1.5	107.3	51.14	1276	3	1397	3	24.95	27.32	1.095
4	100	0.5	23.85	229.9	2172	4	3839	4	9.447	16.70	1.767
5		1.0	95.39	107.4	2385	4	2807	4	22.20	26.12	1.177
6		1.5	214.6	70.07	2005	3	2248	3	28.61	32.08	1.121
7		2.0	381.6	51.81	1673	3	1645	3	32.30	31.76	0.983
8	250	0.5	59.62	345.9	5887	6	8147	7	17.02	23.55	1.384
9		1.0	238.5	166.8	4766	5	5059	5	28.57	30.33	1.061
10		1.5	536.6	109.3	3844	4	3774	4	35.17	34.53	0.982
11		2.0	953.9	82.14	3044	4	2757	4	37.06	33.57	0.906
12		3.0	2146	53.97	2252	3	1954	3	41.72	36.20	0.867
13	500	0.5	119.2	477.2	11060	8	13170	8	23.18	27.59	1.190
14		1.0	477.0	231.7	7819	6	7680	6	33.74	33.14	0.982
15		1.5	1073	153.8	5897	5	5366	5	38.34	34.89	0.910
16		2.0	1908	113.7	4660	5	4083	5	40.97	35.90	0.876
17		3.0	4293	77.05	3230	4	2734	4	41.92	35.48	0.846
18	750	0.6	257.6	476.4	14190	9	14530	9	29.79	30.50	1.024
19		0.7	350.6	406.7	12840	8	12960	8	31.56	31.87	1.010
20		0.8	457.9	354.5	11870	8	11410	8	33.47	32.20	0.962
21		0.9	579.5	313.6	11040	7	10490	8	35.20	33.44	0.950
22		1.0	715.5	281.2	10110	7	9421	7	35.94	33.51	0.932
23	1000	0.5	238.5	661.1	19070	10	20180	11	28.84	30.53	1.058
24		0.6	343.4	547.8	17360	9	17260	10	31.69	31.50	0.994
25		0.7	467.4	466.5	15630	9	15100	9	33.50	32.97	0.966
26		0.8	610.5	406.8	14450	8	13560	9	35.53	33.33	0.938
27		0.9	772.7	360.4	13090	8	12110	8	36.33	33.61	0.925
28		1.0	953.9	323.8	12180	8	11030	8	37.61	34.06	0.906
29		1.5	2146	215.9	8956	7	7814	6	41.49	36.20	0.872
30		2.0	3816	160.4	6881	6	5867	6	42.90	36.70	0.856
31		3.0	8585		4779	5	4029	5			0.843
32	2000	0.4	305.3	1163	35620	14	36150	14	30.80	31.09	1.009
33		0.5	477.0	924.0	31250	13	29920	13	33.82	32.38	0.957
34		0.6	686.8	765.9	27450	12	25490	12	35.84	33.28	0.928
35		0.7	934.9	655.5	24380	11	22170	11	37.19	33.83	0.910
36		1.0	1908	454.9	18520	9	16120	9	40.71	35.45	0.871
37		1.5	4293	301.9	12920	8	10930	8	42.80	36.22	0.846
38		2.0	7632	225.8	9957	7	8308	7	44.09	36.79	0.834
39		3.0	17170	151.6	6912	6	5777	6	45.58	38.10	0.836
40		4.0	30530	112.6	5179	5	4226	5	45.99	37.53	0.816
41		6.0	68680	76.80	3500	4	2806	4	45.58	36.54	0.802
42		10.0	190800	45.21	2150	3	1688	3	47.56	37.35	0.786
43	75	0.65	30.23	150.7	1835	3	2791	4	12.17	18.52	1.521
45	475		191.4	352.7	9575	7	10501	8	27.15	29.77	1.097
46	75	0.80	45.79	120.3	1865	3	2619	4	15.51	21.78	1.404
47	150		91.58	164.4	3612	4	4277	5	21.97	26.02	1.184
48	550		335.8	305.7	9529	7	9622	7	31.17	31.48	1.010

TABLE. 2

GENERAL INSTABILITY PRESSURES OF RING STIFFENED SHELLS
EFFECT of RING GEOMETRY

CASE	SHELL GEOMETRY			RING GEOMETRY			λ_0	λ_{cr}				λ^+/λ_0	λ^-/λ_0	λ^-/λ^+			
	L/R	R/t	Z	A_2/ah	I_{22}/ah^3	$ e_2/h $		UNSTIFFENED	$+e_2$	t	$-e_2$				t		
49	0.5	100	23.85	0.10	1	5	229.9	1355	6	1613	6	5.892	7.017	1.191			
50				0.30	3			1966	4	2907	5	8.549	12.64	1.479			
4				0.50	5			2172	4	3839	4	9.447	16.70	1.767			
51				0.80	8			2466	4	4805	4	10.73	20.90	1.948			
52		1000	238.5	0.05	0.5		661.1	5633	14	4903	14	7.413	7.417	0.974			
53				0.10	1			7805	13	7624	13	11.81	11.53	0.977			
54				0.30	3			14740	11	14950	11	22.29	22.61	1.014			
23				0.50	5			19070	10	20180	11	28.84	30.53	1.058			
55				0.80	8			23890	9	25710	10	36.14	38.90	1.076			
56		1500	357.7	0.05	0.5		804.9	6421	16	6176	16	7.977	7.673	0.962			
57				0.10	1			10010	14	9640	14	13.44	11.98	0.963			
58				0.50	5			25670	11	25380	12	31.89	31.54	0.989			
59				0.80	8			32160	11	32770	11	39.95	40.71	1.019			
60		2000	477.0	0.10	1		924.0	11950	15	11340	16	12.93	12.27	0.949			
61				0.30	3			23490	13	22390	14	25.42	24.23	0.953			
33				0.50	5			31250	13	29920	13	33.81	32.37	0.957			
62				0.80	8			39360	12	38620	12	42.59	41.76	0.981			
63		100	23.85	0.50	5	0	229.9	1852	5			8.056		1			
64						1		1773	5	2042	5	7.712	8.232	1.152			
65						2		1805	5	2343	5	7.849	10.19	1.298			
4						5		2172	4	3839	4	9.447	16.70	1.767			
66						8		2772	3	5508	4	12.06	23.95	1.987			
67		1500	357.7			0	13170	13			16.36		1				
68						0.5	13350	13	13250	13	16.59	16.47	0.993				
69						1	13820	13	13620	13	17.17	16.92	0.986				
70						3		18340	12	17830	13	22.79	22.15	0.972			
58						5		25670	11	25380	12	31.89	31.54	0.989			
71						8		39270	10	41030	11	48.79	50.98	1.045			
72	1.0	50	47.70	0.1	1	5	78.48	632.1	4	669	4	8.054	8.779	1.090			
2				0.5	5			1216	3	1707	3	15.50	21.75	1.404			
73				0.8	8			1527	3	2193	3	19.46	27.94	1.436			
74		100	95.39	0.1	1		107.4	1063	5	1095	5	9.898	10.20	1.030			
5								0.5	5		2365	4	2807	4	22.20	26.12	1.177
75								0.8	8		2912	3	3664	4	27.11	34.11	1.258
76		200	190.8	0.05	0.5		148.6	1127	7	1101	7	7.582	7.407	0.977			
77								0.10	1		1685	6	1669	6	11.33	11.25	0.991
78								0.50	5		4137	5	4371	5	27.84	29.41	1.057
79								0.80	8		5135	4	5731	5	34.55	38.56	1.116
80		300	286.2	0.05	0.5		180.4	1418	7	1379	7	7.861	7.645	0.972			
81								0.10	1		2206	7	2131	7	12.23	11.81	0.966
82								0.50	5		5542	5	5731	6	30.72	31.77	1.034
83								0.80	8		6804	5	7273	5	37.72	40.32	1.069
84		400	381.6	0.05	0.5		207.2	1662	8	1597	8	8.020	7.71	0.961			
85								0.10	1		2617	7	2517	7	12.65	12.15	0.962
86								0.50	5		6694	6	6582	6	32.30	31.76	0.983
87								0.80	8		8710	6	8586	6	42.03	41.31	0.983

TABLE 2 (contd.)

GENERAL INSTABILITY PRESSURES OF RING STIFFENED SHELLS
EFFECT OF RING GEOMETRY

CASE	SHELL GEOMETRY			RING GEOMETRY			λ_0 UNSTIFFENED	$\lambda_{1,r}$				λ^1/λ_0	λ^-/λ_0	λ^-/λ^1				
	L/R	R/h	Z	λ_2 ah	$l_{2,2}$ ah	$l_{e,2}$ h		σ_2		$-\sigma_2$								
								inside	t	outside	t							
88	1.0	500	477.0	0.1	1	5	231.7	2991	8	2835	8	12.91	12.23	0.948				
89				0.3	3			5914	7	5599	7	25.52	24.16	0.947				
14				0.5	5			7819	6	7680	6	33.74	33.14	0.982				
90				0.8	8			9841	6	9654	6	42.46	41.66	0.981				
91		2000	1908	0.8	8		323.8	23790	9	20600	9	52.31	45.29	0.866				
122		50	47.7	0.5	5	1	78.48	879.1	3	958.1	4	11.20	12.21	1.090				
2						5		1216	3	1707	3	15.50	21.75	1.404				
92						8		1711	2	2721	3	21.80	34.67	1.590				
93		100	95.39			1	107.4	1472	4	1556	4	13.70	14.48	1.057				
5						5		2385	4	2807	4	22.20	26.12	1.177				
94						8		3232	3	4691	4	30.09	43.67	1.451				
95	1.0	600	572.4	0.5	5	0	252.8	4347	8			17.20		1				
96												4436	8	4367	8	17.55	17.28	0.984
97											0.5	4633	8	4496	8	18.33	17.79	0.970
98											1	8882	7	8335	7	35.14	32.98	0.938
99											5	11210	6	10990	6	44.33	43.47	0.980
100											5.5	12740	6	13470	6	54.35	53.29	0.980
101											8							
102		2000	1908			8	323.8	30160	9	26340	9	66.29	57.90	0.873				
103	2.0	1000	3816	0.05	0.5	5	160.4	1496	7	1380	7	9.225	8.602	0.923				
104				0.10	1			2380	7	2158	7	14.84	13.46	0.907				
30				0.3	3			4959	6	4274	6	30.92	26.65	0.862				
105				0.5	5			6881	6	5887	6	42.90	36.70	0.856				
				0.8	8			9227	5	7682	5	57.53	47.89	0.833				
106						0.5		5	0	3166	6			19.74		1		
107									0.5	3248	6	3149	6	20.25	19.63	0.969		
108									1	3394	5	3195	6	21.16	19.92	0.941		
109									3	4622	6	4026	6	28.82	25.10	0.871		
30									5	6881	6	5887	6	42.90	36.70	0.856		
110									6.5	9183	5	7681	5	57.25	47.89	0.837		
111					8	11260	5	9416	5	70.22	58.70	0.836						
112	1.0	700	667.8	0.1	1	1	272.1	1685	10	1641	10	6.193	6.032	0.974				
113				0.3	3	3		4935	8	4603	8	18.14	16.91	0.933				
114				0.8	8	8		18910	6	18500	6	69.51	67.97	0.978				
115																		
116		800	763.2	0.1	1	1	290.9	1815	10	1765	10	6.839	6.067	0.972				
117				0.3	3	3		5385	8	5005	8	18.51	17.21	0.929				
118				0.8	8	8		20800	6	20320	6	71.50	69.86	0.977				
119		900	858.5	0.1	1	1	307.8	1949	11	1896	11	6.330	6.159	0.973				
120				0.3	3	3		5783	9	5338	9	18.79	17.34	0.923				
				0.8	8	8		22930	6	21570	7	74.48	70.07	0.941				
121	2.5	2000	11930	1	0	10		22600	5	16650	5			0.746				

TABLE.3
EFFECT of ECCENTRICITY on BUCKLING ~~IN~~ PRESSURE
(LATERAL & HYDROSTATIC)

Typical Cases

$$A_2/ah = 0.5 \quad I_{22}/ah^3 = 5 \quad e_2/h = \pm 5$$

CASE	L/R	R/h	Z	λ_{cr} (HYDROSTATIC)		λ^-/λ^+	λ_{cr} (LATERAL)		λ^-/λ^+
				+ e_2 inside	- e_2 outside		+ e_2 inside	- e_2 outside	
1	0.5	50	11.98	896.8	1768	1.972	2803	4664	1.664
4		100	23.85	2172	3839	1.767	4589	6997	1.525
8		250	59.62	5887	8147	1.384	9094	11430	1.257
13		500	119.2	11060	13170	1.190	14470	16410	1.134
23		1000	238.5	19070	20180	1.058	22830	23470	1.028
33		2000	477	31250	29920	0.957	34898	33410	0.957

TABLE. 4

EFFECT OF POISSON'S RATIO ON THE ECCENTRICITY EFFECT

$$I_{22}/ah^3 = 5 \quad A_2/ah = 0.5 \quad e_2/h = \pm 5$$

R/h	L/R	ν	λ_{cr}		λ^-/λ^+
			+e ₂ inside	-e ₂ outside	
250	0.5	0	6162	9797	1.590
		0.3	5887	8147	1.384
		0.5	5037	6383	1.267
2000	2.0	0	9722	10081	1.037
		0.3	9957	8308	0.834
		0.5	9055	6497	0.717

TABLE. 5

CRITICAL PRESSURES FOR STRINGER AND RING STIFFENED SHELLS

$$\text{RING GEOMETRY : } A_2/ah = 0.5 \quad I_{22}/ah^3 = 5 \quad e_2/h = \pm 5$$

$$\text{STRINGER GEOMETRY : } A_1/bh = 0.5 \quad I_{11}/bh^3 = 5 \quad e_1/h = \pm 5$$

R/h	L/R	Z	λ_0 UNSTIFF.	RING STIFFENED			STRINGER STIFFENED		
				λ^+/λ_0	λ^-/λ_0	λ^-/λ^+	λ^+/λ_0	λ^-/λ_0	λ^-/λ^+
50	0.5	11.92	173.2	5.177	10.21	1.971	6.271	6.424	1.024
100	1.0	95.39	107.4	22.20	26.12	1.177	2.369	2.804	1.184
	1.5	214.6	70.07	28.61	32.08	1.121	1.587	2.109	1.329
	2.0	381.6	51.81	32.29	31.75	0.983	1.282	1.802	1.406
2000	2.0	17170	151.6	45.58	38.10	0.834	1.048	1.162	1.109

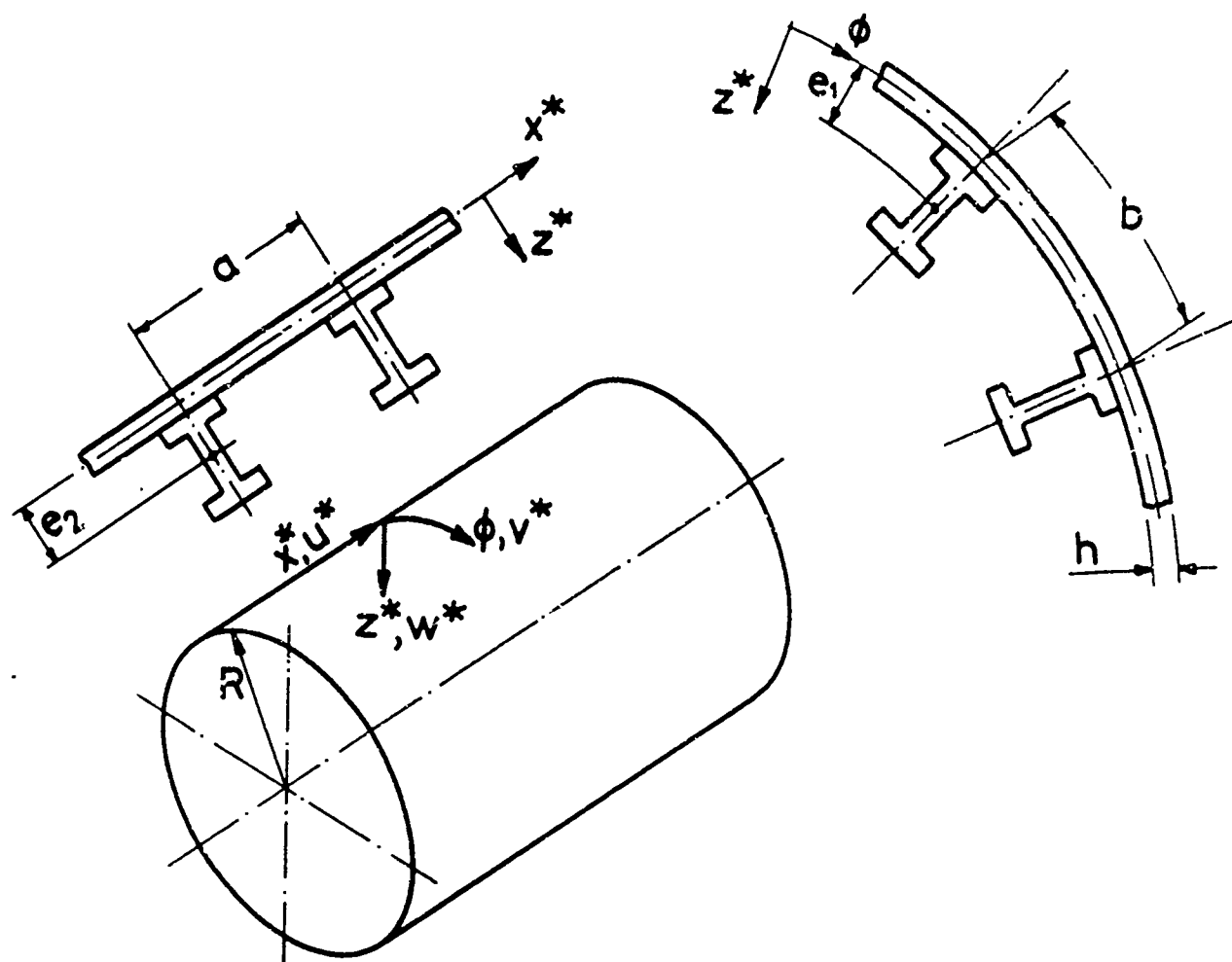


FIG. 1 NOTATION

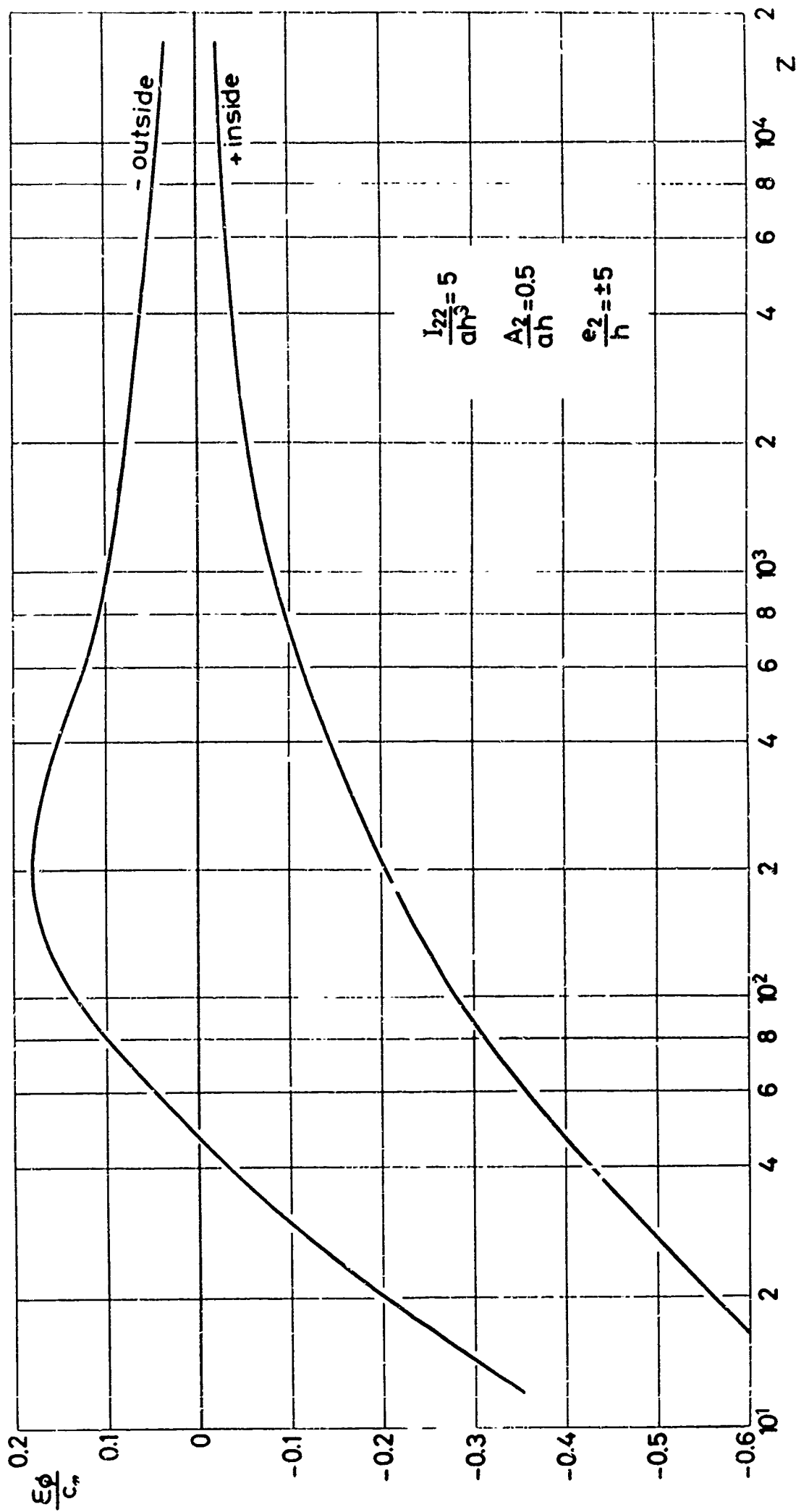


FIG.2 VARIATION OF CIRCUMFERENTIAL STRAIN WITH SHELL GEOMETRY

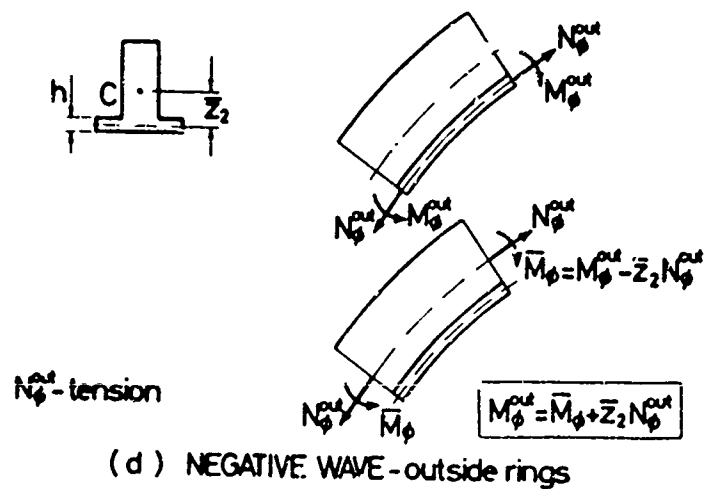
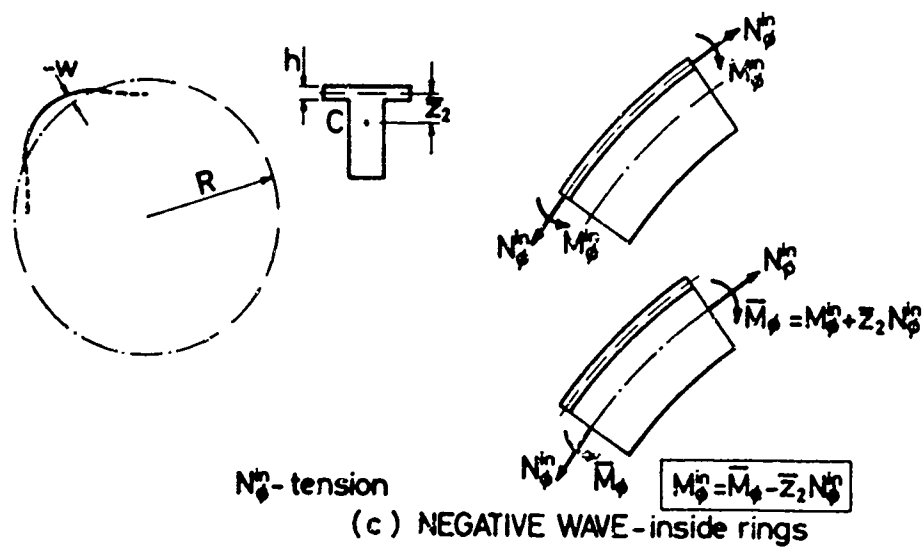
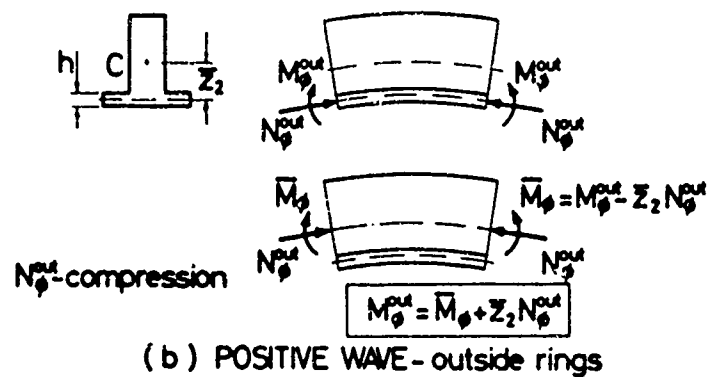
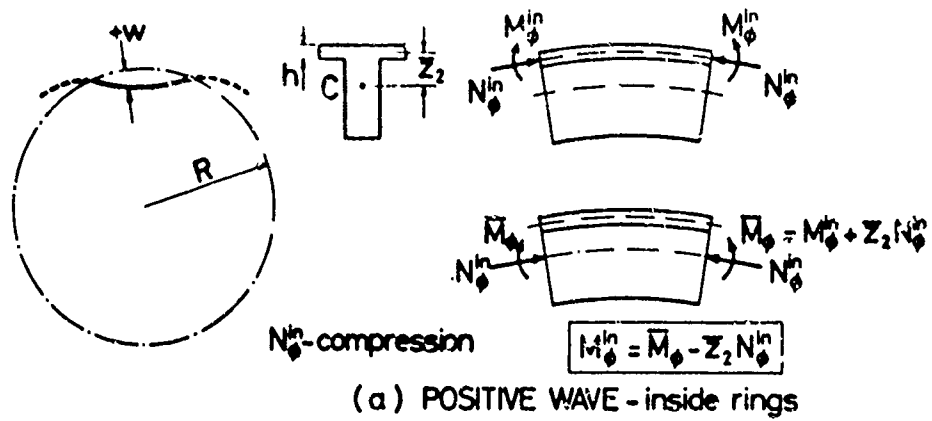
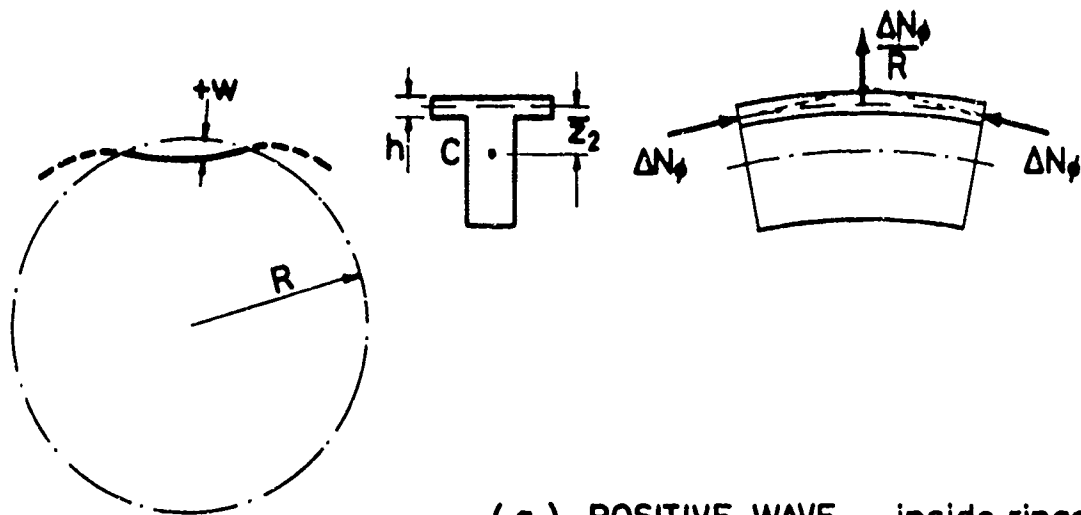
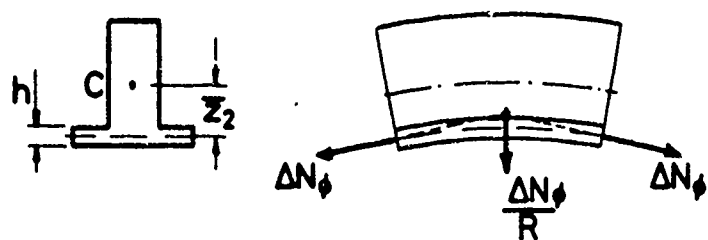


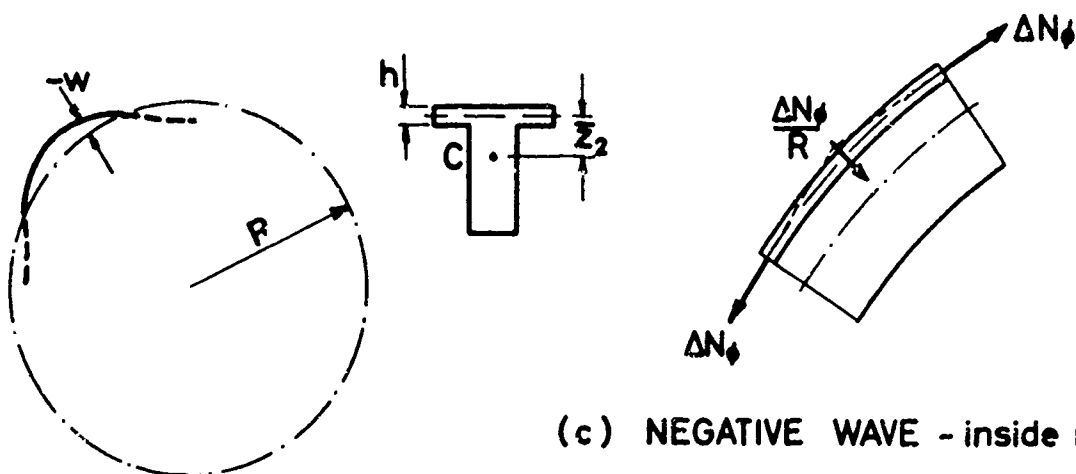
FIG. 3



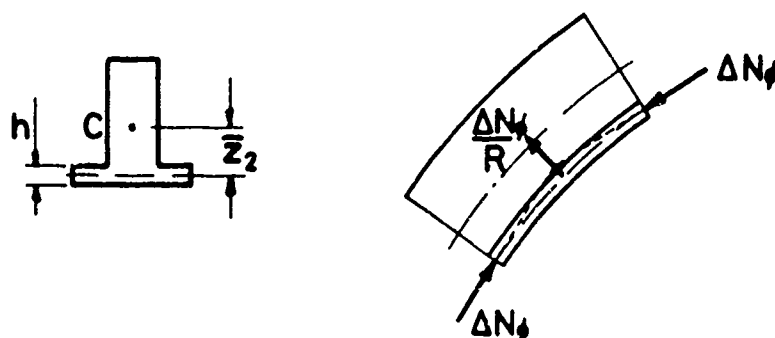
(a) POSITIVE WAVE - inside rings



(b) POSITIVE WAVE - outside rings



(c) NEGATIVE WAVE - inside rings



(d) NEGATIVE WAVE - outside rings

FIG. 4

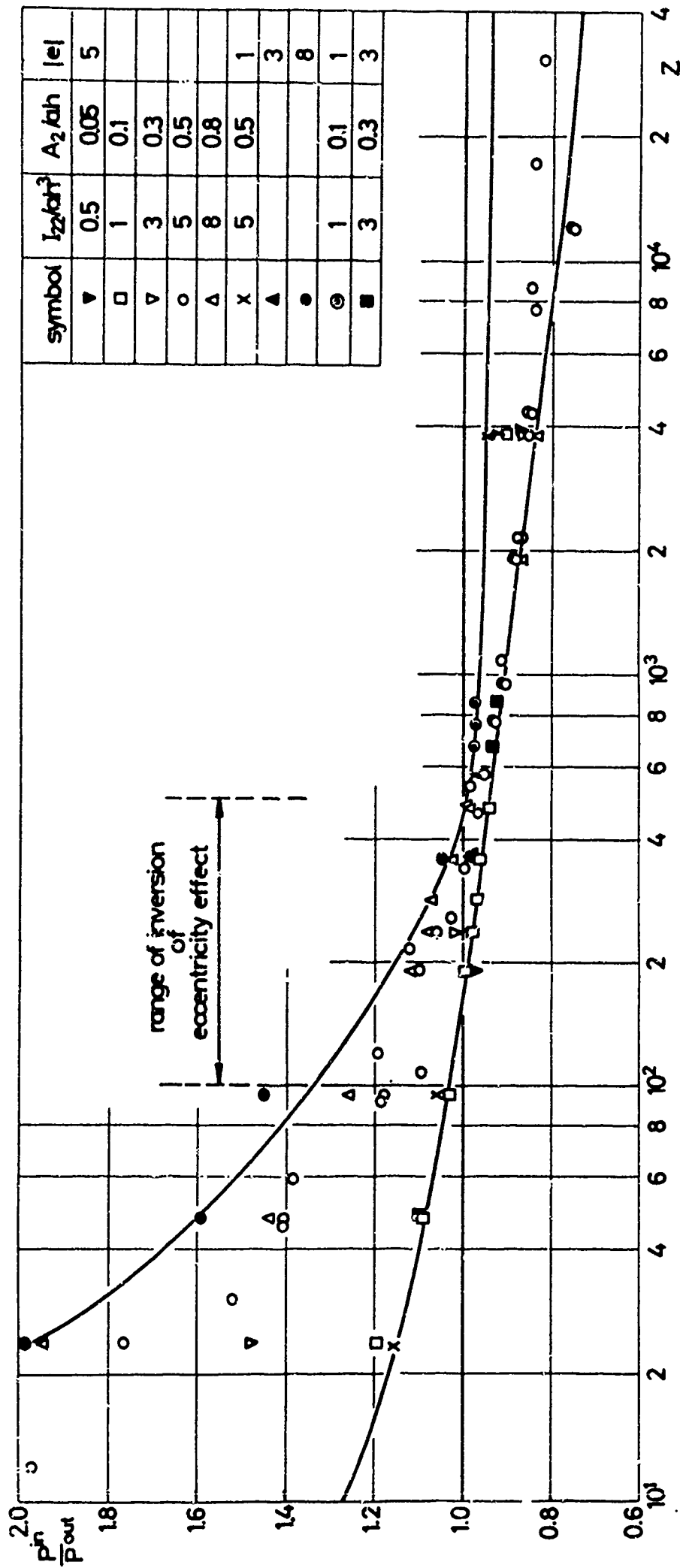


FIG. 5 VARIATION OF ECCENTRICITY EFFECT WITH SHELL PARAMETER Z

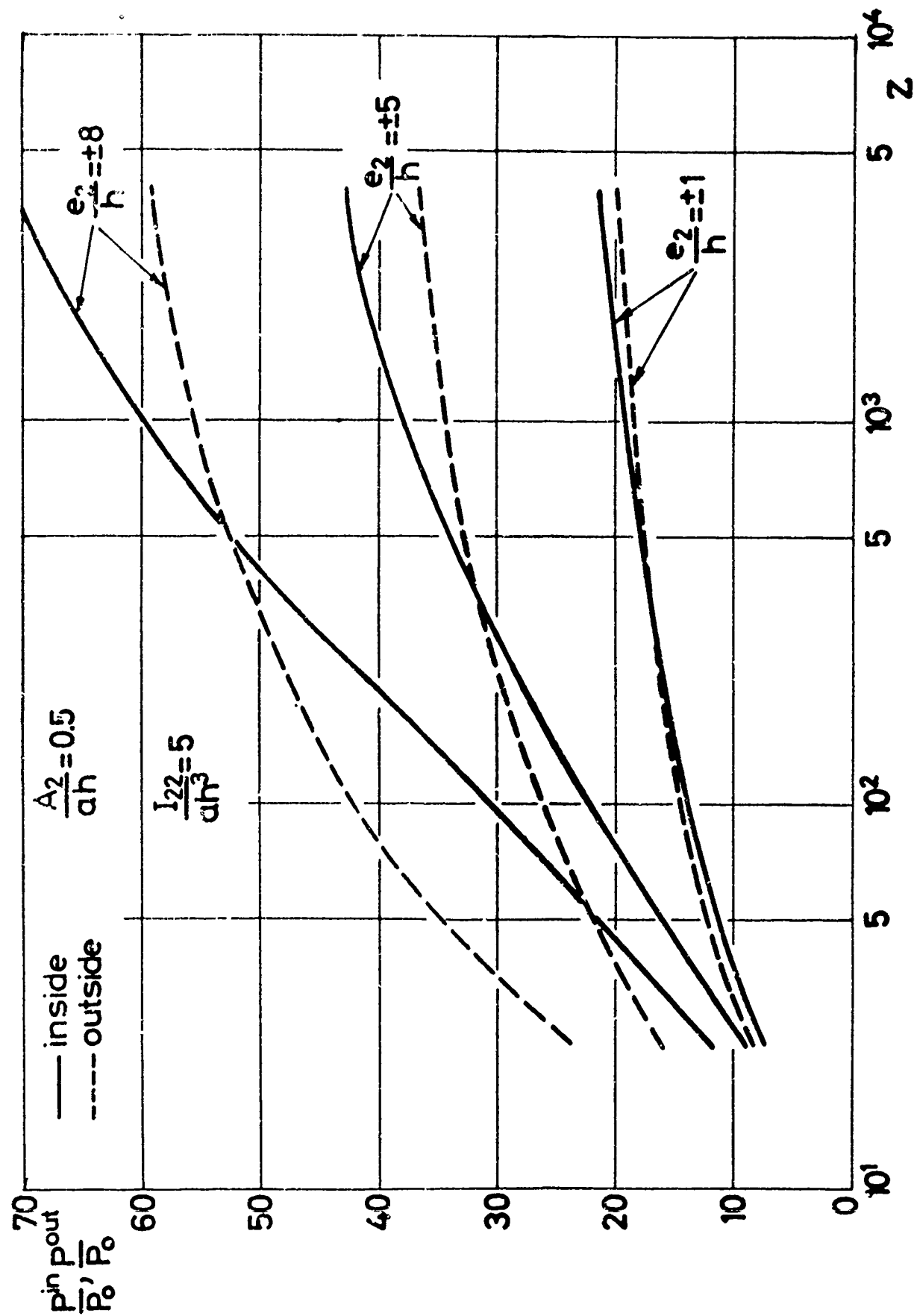


FIG. 6 EFFECT OF MAGNITUDE OF ECCENTRICITY ON STIFFENING
 OF SHELL

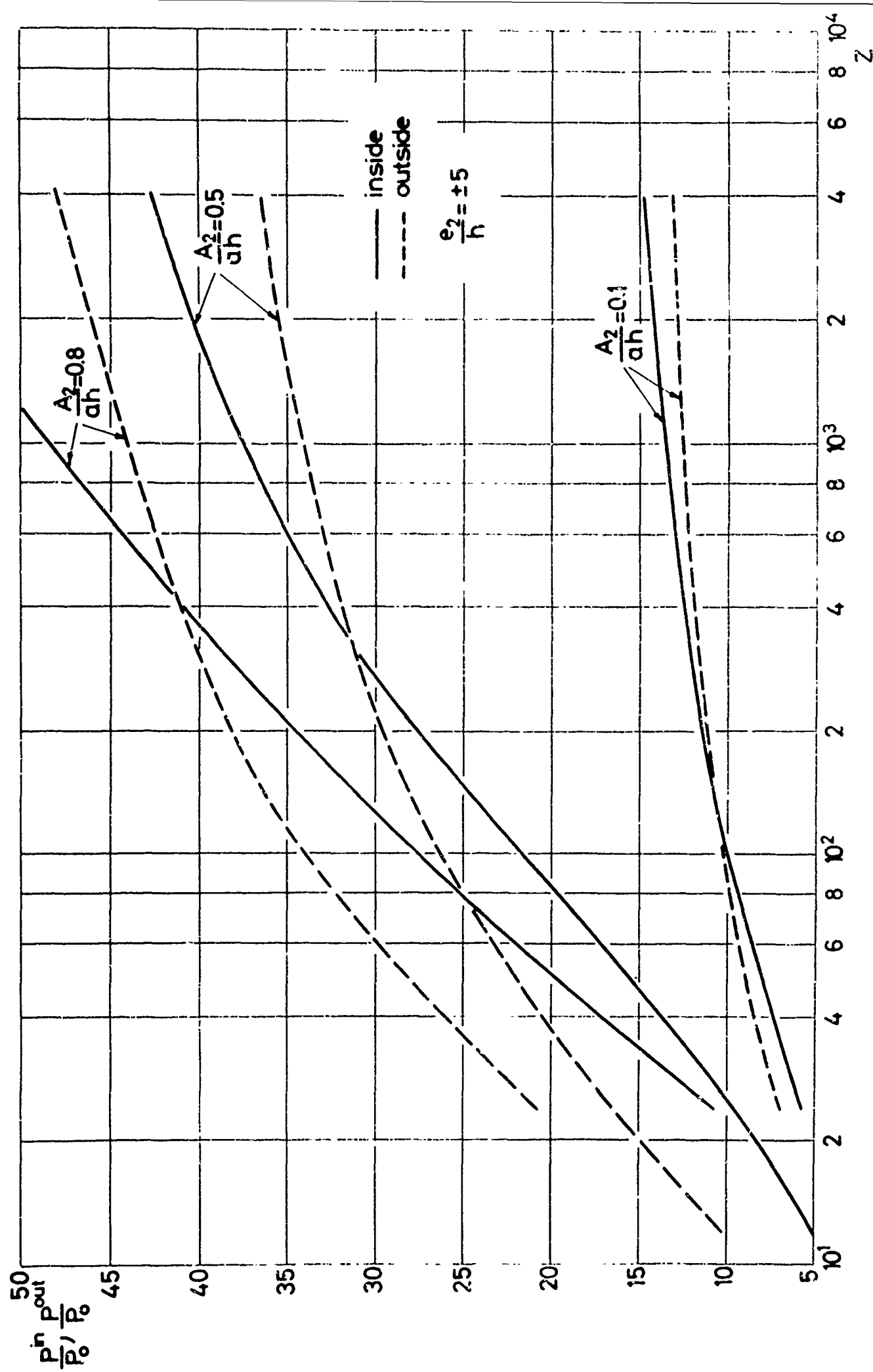


FIG. 7 INFLUENCE OF RING AREA AND MOMENT OF INERTIA ON STIFFENING OF SHELL

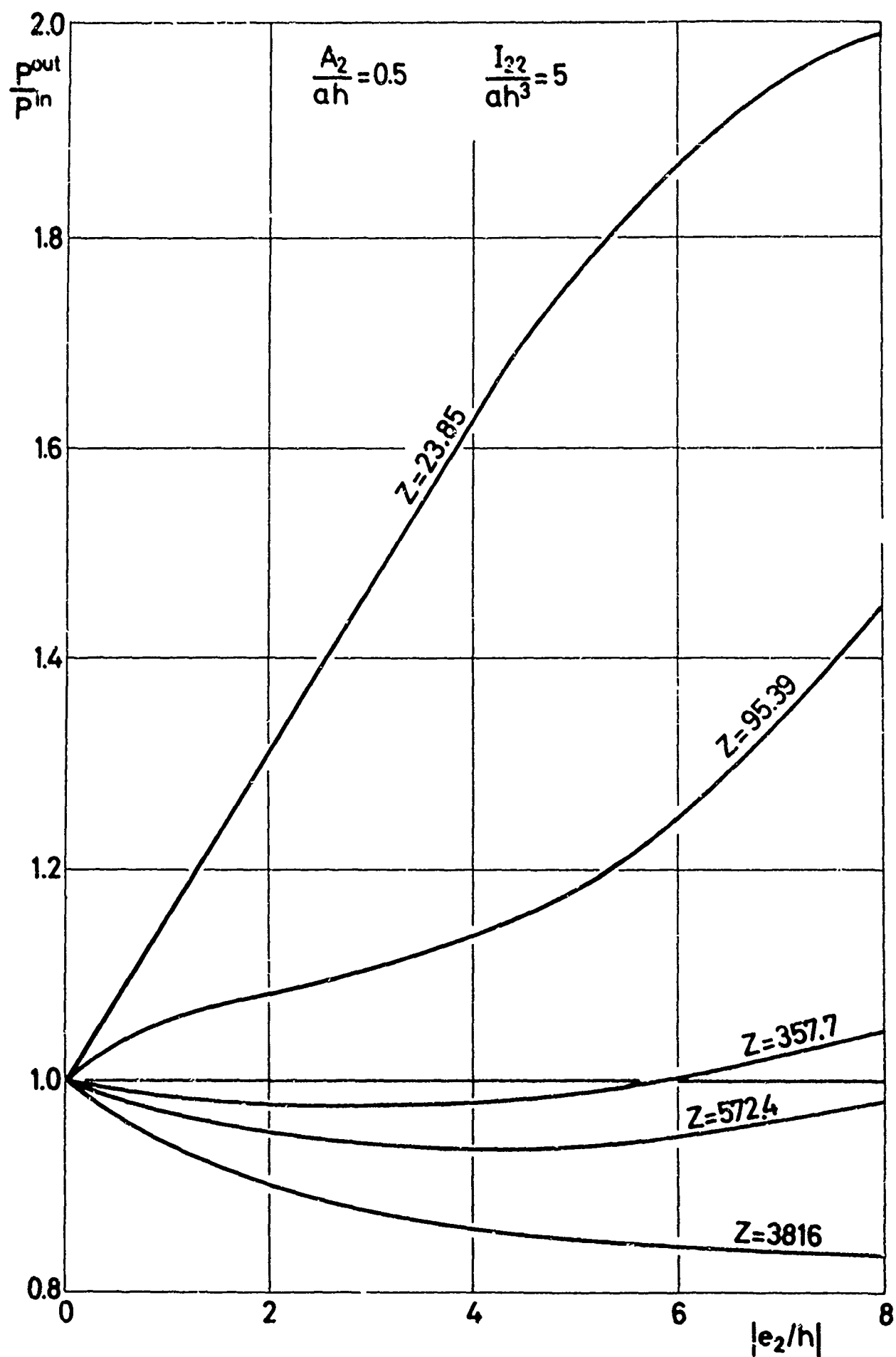


FIG. 8 VARIATION OF ECCENTRICITY EFFECT WITH MAGNITUDE OF ECCENTRICITY

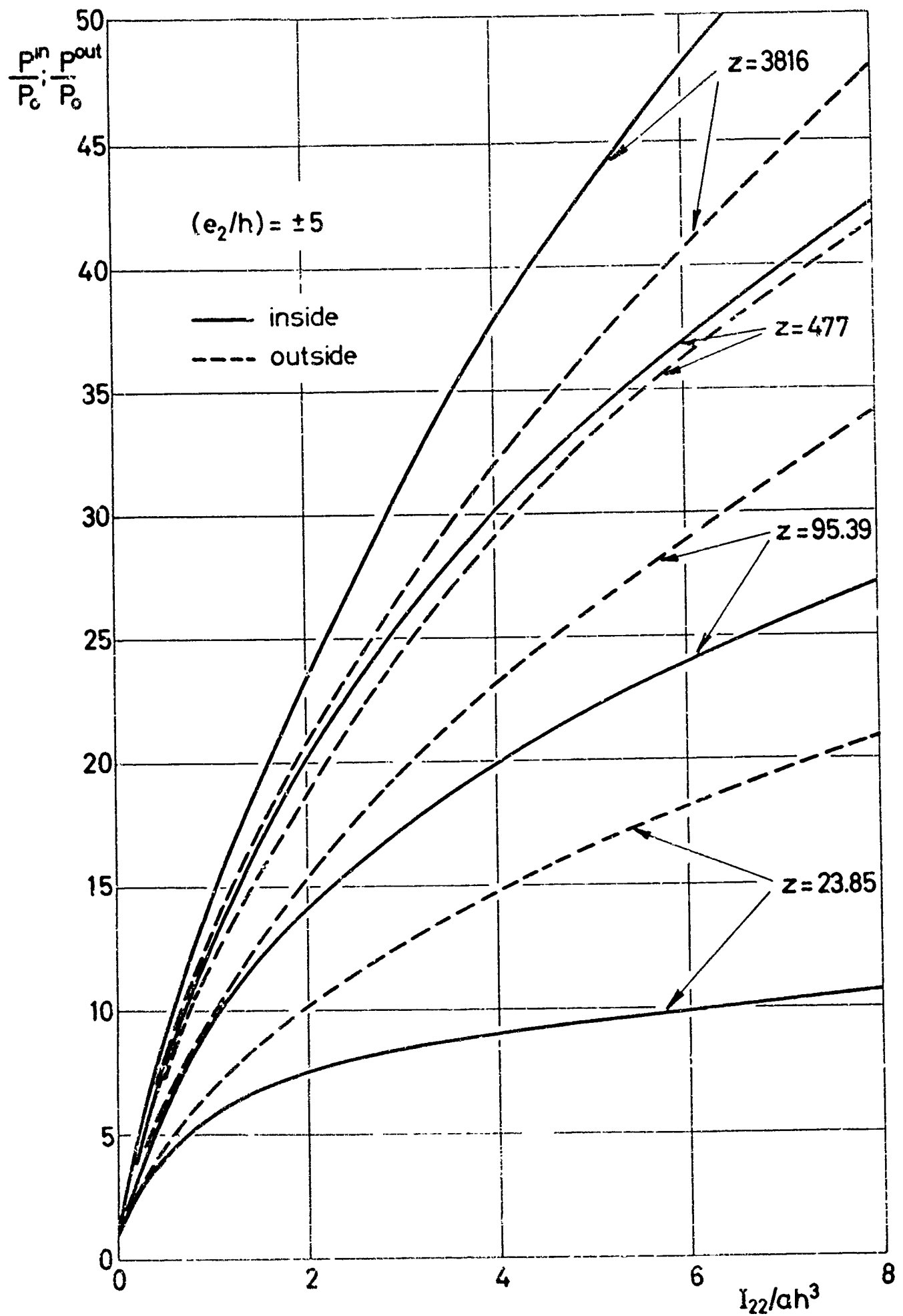


FIG. 9 VARIATION OF STIFFENING OF SHELL WITH RING AREA AND MOMENT OF INERTIA